

Full Paper

Lantabetulic Acid Derivatives Induce G1 Arrest and Apoptosis in Human Prostate Cancer Cells

Kai-Wei Lin¹, Zih-You Lin¹, A-Mei Huang², Jing-Ru Weng³, Ming-Hong Yen⁴, Shyh-Chyun Yang^{1*}, and Chun-Nan Lin^{1,3}

¹ Faculty of Fragrance and Cosmetics, College of Pharmacy, Kaohsiung Medical University, Kaohsiung, Taiwan

² Institute of Biochemistry, College of Medicine, Kaohsiung Medical University, Kaohsiung, Taiwan

³ Department of Biological Science and Technology, School of Medicine, China Medical University, Taichung, Taiwan

⁴ Institute of Natural Product, College of Pharmacy, Kaohsiung Medical University, Kaohsiung, Taiwan

Ten new lantabetulic acid (**1**) derivatives **2–11** were synthesized and their cytotoxicities against human prostate cancer cells were evaluated. PC3 cells treated with 10 μM **8** exhibited the most potent G1 phase arrest. In addition, 10 μM **8** markedly decreased the levels of cyclin E and cdk2 and caused an increase in the p21 and p27 levels, while 20 μM **8** mainly led to cell death through the apoptotic pathway, which correlated with an increase in reactive oxygen species levels, decreased expression levels of Bcl-2 and caspase-8, the induction of mitochondrial changes, and decreased levels of cytochrome *c* in mitochondria. The dual action of **8** could provide a new approach for the development of chemotherapeutic drugs.

Keywords: Apoptosis / Cytotoxicity / G1 arrest / Lantabetulic acid / Synthesis

Received: June 13, 2013; Revised: August 30, 2013; Accepted: September 5, 2013

DOI 10.1002/ardp.201300224

Introduction

Prostate cancer is the most often diagnosed cancer and the most common malignant tumor in men in the Western countries [1]. Current therapies, including radical prostatectomy, local radiotherapy, or brachytherapy, have limited efficacy against the metastatic disease [2]. Consumption of plant-derived foods such as polyphenolic phytochemicals with potent antioxidant activity may reduce the incidence of prostate cancer [3]. Indeed, there has been an increase in the use of dietary plant-derived food to prevent or treat cancer. Hence, the development of plant-derived natural products with strong antioxidant activity could appreciably reduce the disease-related mortality.

Natural or semisynthetic triterpenoids have attracted much interest because of their structural diversity and their broad spectrum of pharmacological activities, such as anti-inflammatory, gastroprotective, antimicrobial, antinocicep-

tive, antioxidant, analgesic, cytotoxic, and antidepressive effects [4]. Recently, a large number of synthetic derivatives of natural triterpenoids have contributed to the pharmacological characterization of these compounds [4].

Recently, we have reported several series of natural triterpenoid derivatives and evaluated them as potent anticancer agents [5, 6]. In addition, it has been reported that the natural triterpenoid lantabetulic acid (**1**), which is structurally different from other types of triterpenoids, causes NUGC-3 and HONE-1 cells to show survival rates of 10% and 38%, respectively [7]. However, a report on a series of structures of lantabetulic acid derivatives in relationship to their cytotoxic activities has so far not appeared in the literature. Therefore, we synthesized a series of lantabetulic acid derivatives, evaluated their cytotoxic effects against the human prostate cancer cell line PC3, and discussed their structure–cytotoxicity relationships. In this study, we also reported the possible mechanism of induced cell death of the selective compound **8**.

Correspondence: Chun-Nan Lin, Faculty of Fragrance and Cosmetics, College of Pharmacy, Kaohsiung Medical University, Kaohsiung 80708, Taiwan.

E-mail: lincna@cc.kmu.edu.tw

Fax: +886 7 5562365

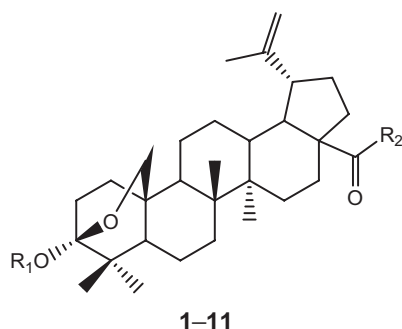
*Additional correspondence: Shyh-Chyun Yang,
E-mail: scyang@kmu.edu.tw

Results and discussion

Chemistry

To increase the anticancer activity of **1** isolated from the roots of *Rhus javanica* L. var. *roxburghiana*, various **1** derivatives were synthesized through chemical modification at the carboxylic acid group at C-17 and the alcoholic group at C-3 (Table 1 and Scheme 1). The C-17-COOH of **1** in anhydrous CHCl_3 was esterified with trimethylsilyldiazomethane (TMSCHN_2) at room temperature to yield **2**, while the C-17-COOH of **1** in acetone was treated with K_2CO_3 , different alkyl halides or benzyl halide, or 2-chloroethanol or α -monochlorohydrin, and refluxed for 24 h at 80°C , to yield compounds **3–8**. In turn, the C-3-OH of **1** in anhydrous pyridine was reacted with different anhydrides of carboxylic acid or different carboxylic acids and refluxed at 80°C for 24 h, to yield compounds **9–11**. The characterization of the known compound **1** by ^1H NMR has been reported in the literature [7, 8]. For further identification of its structure, the

Table 1. Cytotoxicity (ED_{50} values in μM)^{a)} of lantabetulic acid derivatives.



Compd.	R ₁	R ₂	PC3
1	H	OH	22.09 ± 1.38
2	H	OCH ₃	16.21 ± 1.21
3	H	OCH ₂ CH ₃	12.86 ± 2.31
4	H	O(CH ₂) ₂ OH	21.36 ± 4.29
5	H	OCH ₂ CHOHCH ₂ OH	19.34 ± 1.86
6	H	O(CH ₂) ₂ CH ₃	7.02 ± 2.23
7	H	OCH(CH ₃) ₂	10.36 ± 1.07
8	H	OCH ₂ C ₆ H ₅	6.80 ± 2.97
9	COCH ₃	OH	21.93 ± 2.96
10	COCH ₂ CH ₃	OH	14.44 ± 1.51
11	COCH=CHCH ₃	OH	9.51 ± 2.41
Cisplatin			4.56 ± 0.76

^{a)} Cytotoxicity was assayed by the MTT assay after treating with various concentrations of compounds for 72 h. Data were presented as means ± SD ($n = 5$). Compounds **1–11** or cisplatin dissolved in DMSO were diluted with culture medium containing 0.1% DMSO, respectively. The cultured cells were treated with culture medium containing 0.1% DMSO. Cisplatin was used as a positive control.

^{13}C NMR spectrum of **1** (Table 2) was assigned by 1D and 2D NMR techniques and is reported in this study.

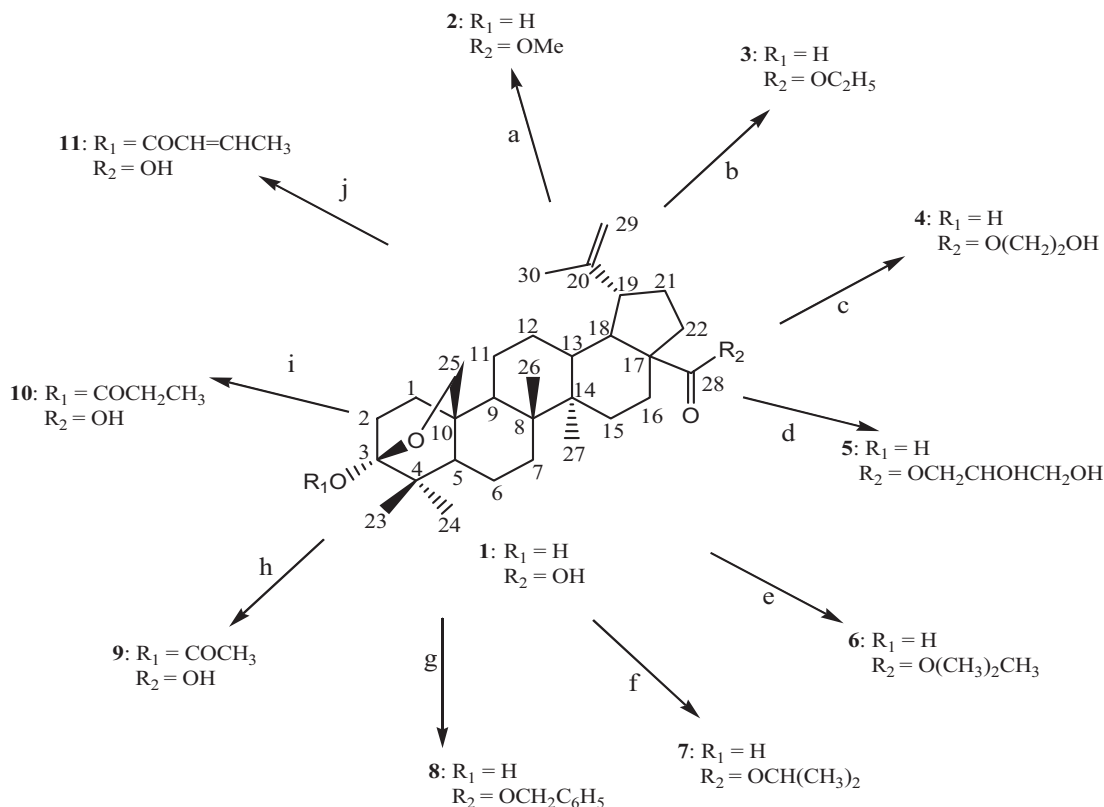
The ^1H NMR spectrum of **2** exhibited proton signals for five tertiary methyls at δ 0.83 (3H, s, Me-26), 0.94 (6H, s, Me-24 and Me-27), 1.01 (3H, s, Me-23), and 1.67 (3H, s, Me-30), a methine proton signal at δ 2.97 (1H, dt, $J = 10.8, 4.4$ Hz, H_β -19), a methyl ester group at δ 3.65 (3H, s, COOCH_3), and two methylene proton signals at δ 3.71 (1H, d, $J = 8.8$ Hz, H_α -25), 4.22 (1H, d, $J = 8.8$ Hz, H_β -25), 4.60 (1H, brs, H_α -29), and 4.72 (1H, brs, H_β -29). The above ^1H and ^{13}C NMR spectra of **2** were almost identical to the corresponding proton and carbon signals of **1** (Table 2), except for the appearance of an additional methyl ester of proton and carbon signals at δ 3.65 and 51.3 in the spectrum of **2**, respectively. In addition, the chemical shift of C-28 of **2** was downfielded from δ 180.1 to 176.6 compared to that of **1**. The above result supports that the structure of **2** was characterized as shown in Scheme 1. The NMR spectra of **3–8** were similar to the corresponding proton and carbon signals of **2**, except for signals of an ester group substituted at C-17 and the chemical shift of Me-26 of **8** upfielded from δ 0.83 to 0.65 compared to that of **2** (Table 2 and Experimental section). The result also supports that the structures of **3–8** were characterized as shown in Scheme 1.

In turn, the ^1H NMR spectrum of **9** indicated proton signals for five tertiary methyls at δ 0.91 (3H, s, Me-26), 0.93 (3H, s, Me-27), 1.02 (3H, s, Me-24), 1.07 (3H, s, Me-23), and 1.69 (3H, s, Me-30), and an acetyl group at δ 1.94 (3H, s, OAc). The above ^1H and ^{13}C NMR spectra were similar to the corresponding proton and carbon signals of **1** (Table 2 and Experimental section), except for the carbon signals at C-3 and C-23, and presenting an additional acetyl group at δ 1.94 and two carbon signals at δ 20.9 and 171.1. In addition, the chemical shift of C-3 was downfielded from δ 98.4 to 04.7 compared to that of **1** (Table 2). This suggests that the structure of **9** was characterized as shown in Scheme 1. The NMR spectra of **10** and **11** were similar to the corresponding data of **9**, except for the carbon signals of C-3 and C-23, and presenting additional signals of acyl groups substituted at C-3 of **10** and **11** (Table 2 and Experimental section), respectively. The result also supports the characterization of the structures of **10** and **11** as shown in Scheme 1. The IR, EIMS, and HREIMS results also supported the characterization of this series of compounds as shown in Scheme 1 (see Experimental section).

Biology

PC3 cells were treated with various concentrations of **1** and its derivatives **2–11** for 72 h and their effects on cell growth were assessed by MTT assay (Table 1). Growth of the PC3 cells was inhibited by all tested compounds in a concentration-dependent manner, as shown in Table 1.

The alkanoylation at C-3 of **1** with acetic anhydride resulted in stronger cytotoxicity against the PC3 cells than that of **1**,



Scheme 1. Synthesis of lantabetulic acid (**1**) derivatives. Reagents and conditions: (a) $CHCl_3$, $TMSCHN_2$, rt, 1 h; (b) acetone, K_2CO_3 , CH_3CH_2I , reflux, $80^\circ C$, 24 h; (c) acetone, K_2CO_3 , CH_2ClCH_2OH , reflux, $80^\circ C$, 24 h; (d) acetone, K_2CO_3 , α -monochlorohydrine, reflux, $80^\circ C$, 24 h; (e) acetone, K_2CO_3 , $CH_3CH_2CH_2I$, reflux, $80^\circ C$, 24 h; (f) acetone, K_2CO_3 , $(CH_3)_2CHI$, reflux, $80^\circ C$, 24 h; (g) acetone, K_2CO_3 , benzylbromide, reflux, $80^\circ C$, 24 h; (h) pyridine, acetic anhydride, stirring, $60^\circ C$, 24 h; (i) pyridine, propionic acid, stirring, $60^\circ C$, 24 h; and (j) *N,N*-dicyclohexylcarbodiimide (in pyridine), crotonic anhydride, stirring, $60^\circ C$, 24 h.

while an increase in the carbon number of the alkyl chain of aliphatic acids, such as in **10**, appreciably enhanced the cytotoxic effect against PC3 cells, as shown in Table 1. The alkanoylation at C-3 with an unsaturated alkyl chain of aliphatic acids, such as in **11**, significantly enhanced the cytotoxicity against the same cancer cell line (Table 1). In turn, the esterification at C-17 of **1** with $TMSCHN_2$ or alkyl halides resulted in stronger cytotoxicity against PC3 cells than that of **1**, while an increase in the carbon number of the alkyl chain, such as in **3** and **6**, significantly enhanced the cytotoxic effect compared to that of **1** (Table 1). The esterification at C-17 of **1** with a branched alkyl halide, such as in **7**, revealed weaker cell growth inhibition of PC3 cells than after the esterification at C-17 of **1** with the corresponding straight-chain alkyl halide, such as in **6** (Table 1). The esterification at C-17 of **1** with benzyl halide, such as in **8**, revealed the strongest cytotoxicity against PC3 cells in this series of compounds (Table 1). The esterification at C-17 of **1** with 1-chloroethanol or α -monochlorohydrin decreased the cytotoxic effect against PC3 cells

compared to the esterification at C-17 with the corresponding alkyl halide, such as in **4** and **5**.

The above results and discussion obtained from the structure–cytotoxicity relationships suggest that this series of compounds shows cytotoxicity against PC3 cells and that the 3-hydroxy-17-benzyl ester of **1**, such as **8**, exhibited the most potent cytotoxic effects against PC3 cells. This compound could be used as a lead compound for the further design and synthesis of novel anticancer agents.

To further evaluate the cytotoxic effects of derivatives of **1**, the mechanisms of cell death induced by the selective compound **8** were studied *in vitro* in PC3 cells. Treatment of PC3 cells with various concentrations of **8** for different incubation times induced cell death in a concentration-dependent manner, except for PC3 cells treated with $1 \mu M$ **8** for 72 h. Among them, exposure of PC3 cells to **8** for 72 h exhibited the most potent cytotoxic effects (Fig. 1).

The generation of reactive oxygen species (ROS) is part of the mechanism by which most chemotherapeutic agents kill tumor cells [2]. We investigated whether the generation of

Table 2. ^{13}C NMR spectral data for compounds 1–11 (in CDCl_3).

Position	1	2	3	4	5	6	7	8	9	10	11
C-1	35.1	35.6	35.6	35.5	35.5	35.5	35.5	35.5	36.9	36.9	37.0
C-2	29.5	29.7	29.6	29.7	29.7	29.6	29.6	29.6	30.5	30.5	30.5
C-3	98.4	98.3	98.3	98.3	98.3	98.3	98.3	98.3	104.7	104.7	104.7
C-4	40.4	40.3	40.3	40.3	40.3	40.3	40.3	40.3	40.4	40.4	40.4
C-5	49.6	49.7	49.7	49.5	49.5	49.7	49.7	49.7	51.5	51.5	51.5
C-6	19.7	19.6	19.7	19.7	19.7	19.7	19.7	19.7	19.6	19.6	19.6
C-7	32.0	32.0	32.0	31.9	31.9	32.0	31.7	31.9	33.2	33.2	33.1
C-8	39.6	39.6	39.7	39.6	39.6	39.6	39.7	39.6	38.6	40.4	40.4
C-9	45.2	45.2	45.2	45.2	45.2	45.2	45.2	45.2	46.8	46.8	46.8
C-10	35.6	35.2	35.2	35.1	35.1	35.2	35.2	35.5	34.4	34.4	34.4
C-11	22.2	22.2	22.2	22.2	22.2	22.2	22.2	22.1	22.2	22.3	22.1
C-12	25.7	25.8	25.8	25.7	25.8	25.8	25.8	25.8	25.7	25.7	25.7
C-13	38.4	38.4	38.4	38.4	38.4	38.4	38.4	38.3	38.8	38.8	38.8
C-14	42.1	42.1	42.1	42.1	42.1	42.1	42.1	42.1	42.5	42.5	42.5
C-15	29.8	29.6	29.5	29.5	29.5	29.5	29.5	29.5	29.9	29.9	29.9
C-16	32.0	32.1	32.0	32.0	32.0	32.0	32.0	32.0	32.0	32.0	32.0
C-17	56.3	56.5	56.4	56.4	56.7	56.5	56.3	56.5	56.3	56.3	56.3
C-18	49.0	49.2	49.1	49.1	49.1	49.1	49.0	49.1	49.1	49.1	49.1
C-19	46.7	46.8	46.8	46.7	46.7	46.8	46.9	46.7	45.8	45.8	45.8
C-20	150.3	150.4	150.5	150.5	150.5	150.5	150.6	150.4	150.2	150.2	150.2
C-21	30.5	30.6	30.6	30.5	30.5	30.6	30.6	30.5	30.5	30.5	30.5
C-22	36.9	36.9	36.9	36.9	36.9	37.0	37.0	36.8	36.9	36.9	37.0
C-23	26.8	26.9	26.8	26.8	26.8	26.8	26.8	26.8	29.3 ^{a)}	29.3 ^{a)}	29.3 ^{a)}
C-24	19.5	19.4	19.4	19.4	19.4	19.4	19.4	19.4	19.4	19.5	19.5
C-25	67.7	68.0	68.0	67.9	68.0	68.0	68.0	67.5	64.5	64.7	64.6
C-26	16.5	16.2	16.2	16.1	16.2	16.2	16.2	16.0	16.0	16.0	16.0
C-27	14.5	14.3	14.3	14.3	14.3	14.3	14.3	14.3	14.9	14.9	14.9
C-28	180.1	176.6	176.0	176.5	176.5	176.1	176.5	175.7	181.6	182.0	181.8
C-29	109.9	109.6	109.5	109.7	109.7	109.5	109.5	109.6	109.8	109.8	109.8
C-30	19.5	18.4	18.4	18.4	18.4	18.4	18.4	18.4	19.4	19.4	19.4
COOCH_3		51.3									
$\text{COOCH}_2\text{CH}_3$			59.8								
$\text{COOCH}_2\text{CH}_3$			14.3								
$\text{COOCH}_2\text{CH}_2\text{OH}$				61.5							
$\text{COOCH}_2\text{CH}_2\text{OH}$				65.5							
Position	5	6	7	8	9	10	11				
$\text{COOCH}_2\text{CHOHCH}_2\text{OH}$	63.5										
$\text{COOCH}_2\text{CHOHCH}_2\text{OH}$	70.5										
$\text{COOCH}_2\text{CHOHCH}_2\text{OH}$	64.7										
$\text{COOCH}_2\text{CH}_2\text{CH}_3$		65.5									
$\text{COOCH}_2\text{CH}_2\text{CH}_3$		1.64									
$\text{COOCH}_2\text{CH}_2\text{CH}_3$		0.95									
$\text{COOCH}(\text{CH}_3)_2$			66.8								
$\text{COOCH}(\text{CH}_3)_2$			21.7								
$\text{COOCH}(\text{CH}_3)_2$			21.7								
$\text{COOCH}_2\text{C}_6\text{H}_5$				65.7							
$\text{COOCH}_2\text{C}_6\text{H}_5$				121.8 × 2							
$\text{COOCH}_2\text{C}_6\text{H}_5$				128.2 × 2							
$\text{COOCH}_2\text{C}_6\text{H}_5$				128.5							
$\text{COOCH}_2\text{C}_6\text{H}_5$				136.4							
CH_3COO					20.9						
CH_3COO					171.1						
$\text{CH}_3\text{CH}_2\text{COO}$						8.9					
$\text{CH}_3\text{CH}_2\text{COO}$						27.4					
$\text{CH}_3\text{CH}_2\text{COO}$						174.6					
$\text{CH}_3\text{CH}=\text{CHCOO}$							38.9				
$\text{CH}_3\text{CH}=\text{CHCOO}$							130.1				
$\text{CH}_3\text{CH}=\text{CHCOO}$							118.7				
$\text{CH}_3\text{CH}=\text{CHCOO}$							171.1				

^{a)} Signals may be revised.

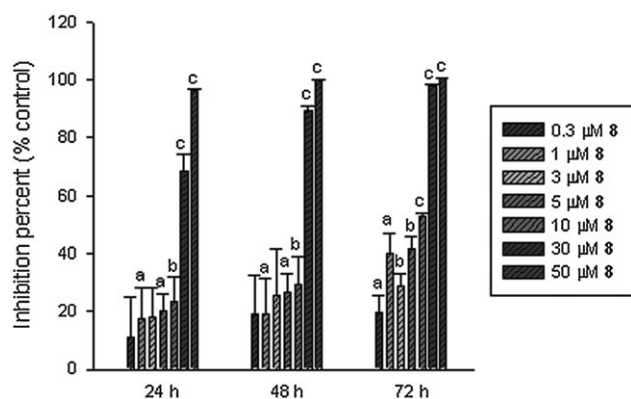


Figure 1. Antiproliferative effects of various concentrations of **8** on PC3 cells. Cells were incubated with various concentrations of **8** and cell growth was determined after 24, 48, and 72 h of treatment. The data shown represent the means \pm SD ($n=5$) for one experiment; $p < 0.05$ (a), $p < 0.01$ (b), and $p < 0.001$ (c) compared to the control values.

intracellular ROS is part of the mechanism by which **8** induces apoptosis in PC3 cells. The generation of ROS by **8** was assessed by the fluorescent dye, H₂DCFDA, which preferentially detects intracellular ROS (Fig. 2). As shown in Fig. 2, exposure of cells to 20 μ M cisplatin and 5, 10, or 20 μ M **8** caused a significant increase in the level of intracellular generation of ROS, while exposure of the cells to 1 mM N-acetylcysteine (NAC) caused a decrease in the level of intracellular ROS. These results indicate that various concentrations of **8** are able to generate intracellular ROS and subsequently induce cell death. This further suggests that the generation of ROS induced by 20 μ M **8** may be correlated with the mechanism by which **8** induces cell death.

Cell cycle arrest and apoptosis are the most common causes of cell growth inhibition. To explore the underlying mechanism of growth suppression induced by **8**, cell cycle analysis was performed by cell sorting of propidium iodide (PI)-stained PC3 cells. As shown in Fig. 3, cells treated with 5 and 10 μ M **8** for 24 h appeared to appreciably accumulate in the G1 phase of the cell cycle, but cells treated with 20 μ M **8** for 24 h showed a significantly increased population of sub-G1

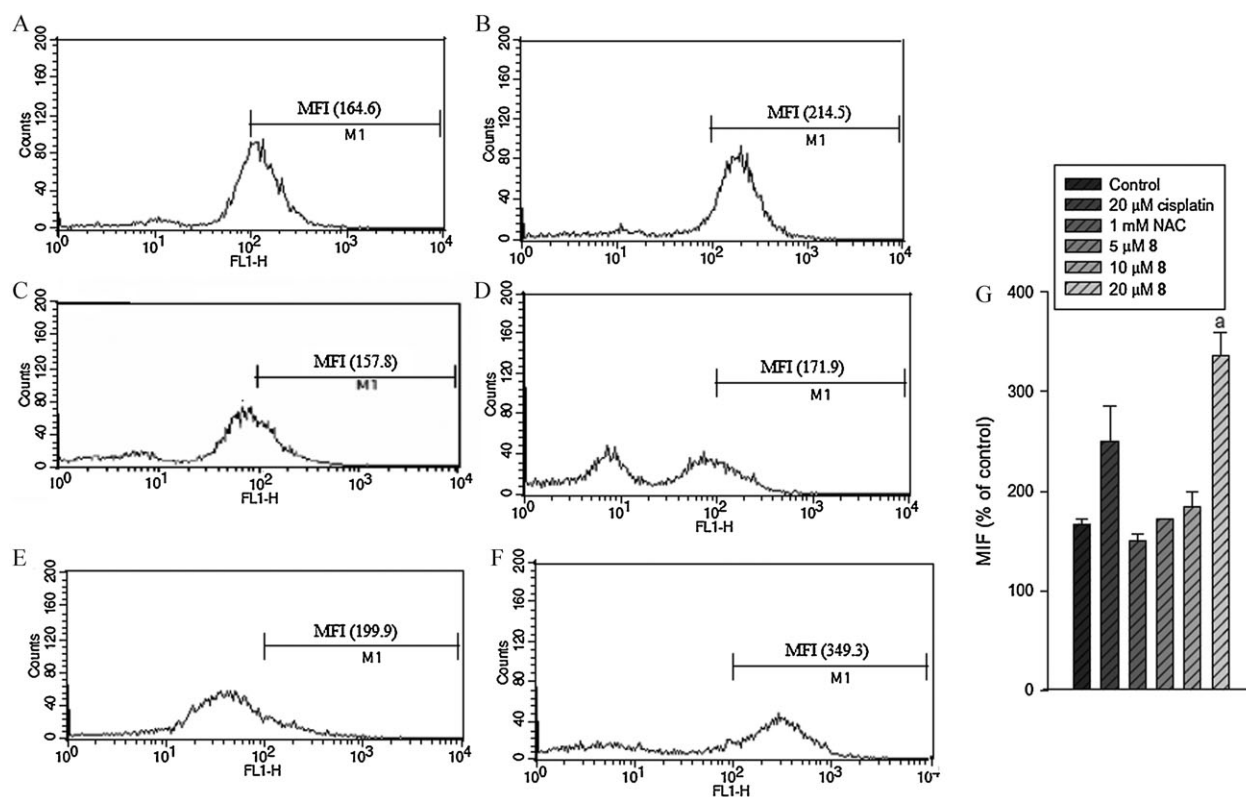


Figure 2. Effects of **8** and cisplatin on the production of ROS in PC3 cells. PC3 cells were treated with (A) control, (B) 20 μ M cisplatin, (C) 1 mM NAC, (D) 5 μ M **8**, (E) 10 μ M **8**, and (F) 20 μ M **8** for 24 h, and the amount of ROS was assayed by H₂DCFDA staining. Each sampling measured the mean fluorescence intensity (MFI) of 3×10^5 cells corrected for autofluorescence. The control cells were treated with vehicle. Similar results were obtained in three repeated experiments. (G) Each bar represents the means \pm SD of the MFI of 3×10^5 cells corrected for autofluorescence from three independent experiments; $p < 0.01$ (a) compared to the respective control value.

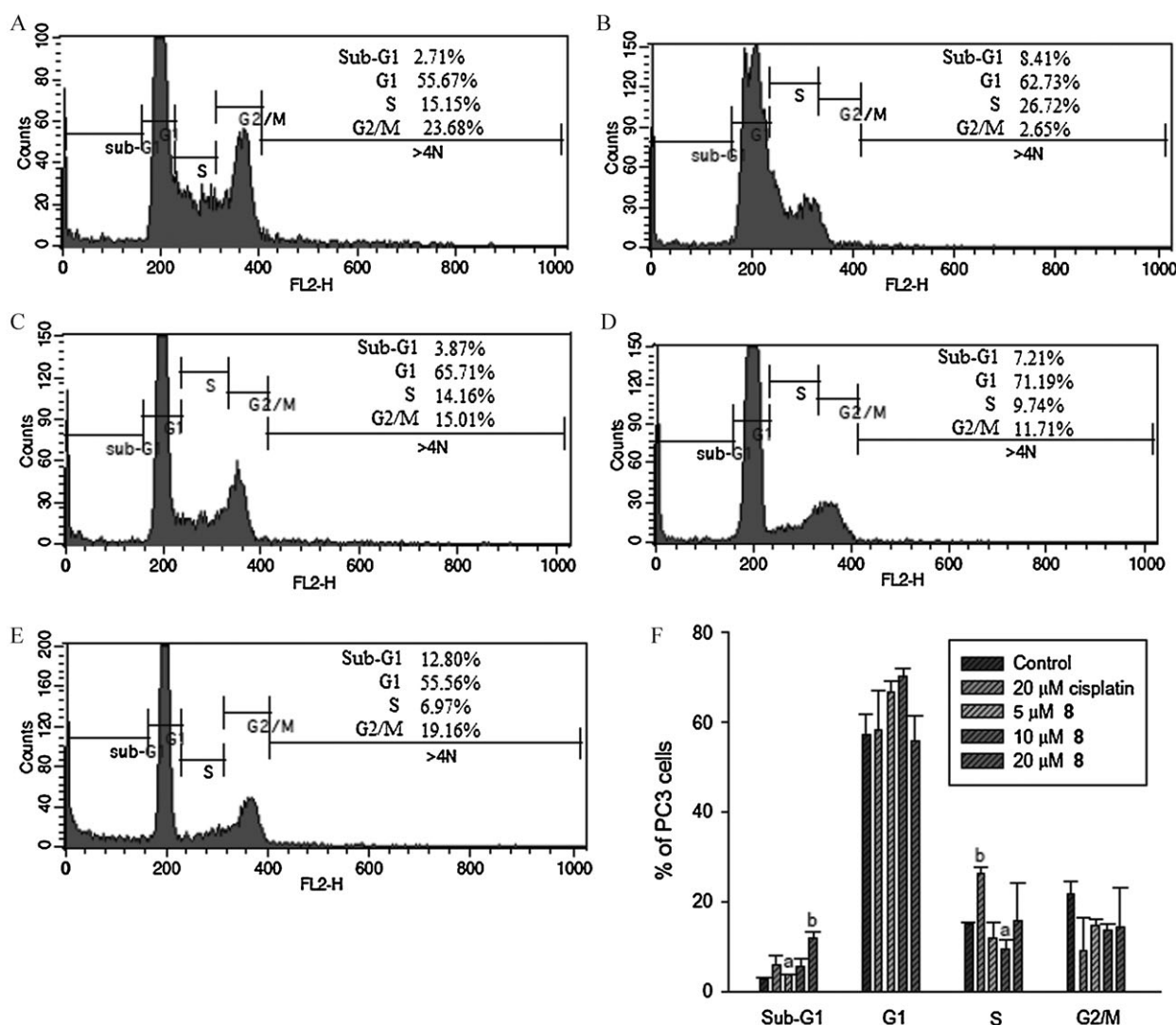


Figure 3. Flow cytometry analysis of PC3 cells treated with cisplatin and **8**. PC3 cells (3×10^5 cells/6-cm dish) were treated with vehicle (control) (A), 20 μ M cisplatin (B), 5 μ M **8** (C), 10 μ M **8** (D), or 20 μ M **8** (E) for 24 h. At the indicated time, cells were stained with PI, and the DNA contents were analyzed by flow cytometry; apoptosis was measured by the accumulation of sub-G1 DNA contents in the cells. The control cells were treated with vehicle. The results are representative of three independent experiments. The bars (F) show the distribution of PC3 cells treated with cisplatin and **8** in the phases of the cell cycle. The values show the percentages of cells in the individual phases of the cell cycle from three independent experiments; $p < 0.05$ (a) and $p < 0.01$ (b) compared to the respective control value.

phase cells, which are apoptotic cells. These results suggest that the induction of cell death by 5 and 10 μ M **8** is mainly due to arresting cells in the G1 phase of the cell cycle, while the induction of cell death by 20 μ M **8** is mainly due to apoptosis.

Induction of cell apoptosis was further confirmed by using a dual staining approach with PI and annexin V-FITC staining. Annexin V-positive/PI-negative (early apoptotic) and annexin V-positive/PI-positive (late apoptotic) cells were increased in PC3 cells treated with **8** for 24 h. The results from the apoptosis assays revealed that the cytotoxicity induced by

20 μ M **8** was due to apoptosis and necrosis (Fig. 4). The number of both early apoptotic and late apoptotic cells was increased about sixfold at 20 μ M **8**, compared to the untreated cells. We also validated that the apoptotic effect of treatment with 20 μ M **8** for 24 h was inhibited by pretreatment with NAC (Fig. 4). This result indicates that ROS generation is required for apoptosis induced by 20 μ M **8**.

It has been suggested that ROS overproduction induced a reduction in the mitochondrial membrane potential (MMP) ($\Delta\psi_m$) as well as mitochondrial dysfunction [9]. Thus, to detect

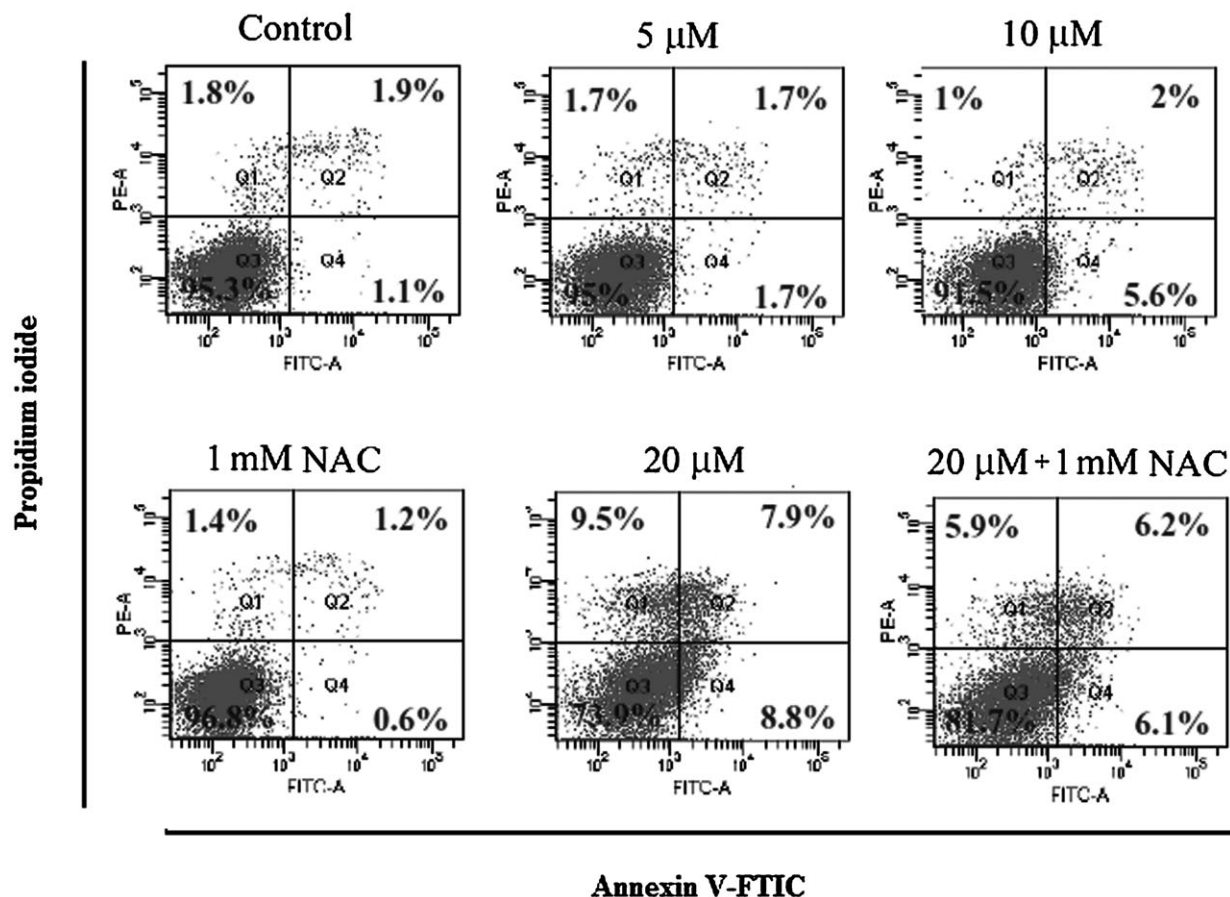


Figure 4. The graphs depict apoptotic and necrotic populations of PC3 cells double stained with PI- and FITC-labeled annexin V. PC3 cells were treated with vehicle (control), 5, 10, or 20 μM **8**, and pre-incubated with 1 mM NAC for 0.4 h prior to exposure to 20 μM **8** for 24 h. The results are expressed as percent of total cells.

changes in the MMP, the specific fluorescent probe JC-1 (5,5',6,6'-tetrachloro-1,1',3,3'-tetraethyl benzimidazolyl carbocyanine iodide) was used. As shown in Fig. 5, the positive control carbonyl cyanide 3-chlorophenylhydrazone (CCCP) and 20 μM **8** significantly increased the number of JC-1 monomers (R2) and decreased that of JC-1 aggregates (R1). This suggests that 20 μM **8** dramatically decreased the $\Delta\psi_m$ in PC3 cells. The marked collapse of the MMP suggests that a dysfunction of mitochondria is involved in the oxidative burst and apoptosis induced by 20 μM **8**. Hence, we demonstrated that 20 μM **8** induced cell death in PC3 cells mainly by apoptosis through the mitochondria-mediated pathway.

Regulation of cell cycle progression in cancer cells is considered to be a potentially effective mechanism for growth control [10]. Since treatment of cells with 10 μM **8** for 24 h exhibited the most potent G1 phase arrest, we next determined the expression of cell cycle-related protein levels by 10 μM **8**. The expression of the cyclin-dependent kinase 2

(cdk2) inhibitors, p21 and p27, which regulate the progression of cells in the G1 phase of the cell cycle, was assessed. The protein levels of p21 and p27 were increased following treatment with 10 μM **8** for 24 h (Fig. 6A). In addition, the expression levels of the G1 positive regulators, cdk2 and cyclin E, were down-regulated following treatment with 10 μM **8** for 24 h (Fig. 6A). This indicates that the G1 arrest induced by 10 μM **8** might be mediated through the up-regulation of the p21 and p27 proteins, which enhance the formation of heterotrimeric complexes with G1-S cyclin-dependent kinases and cyclins, thereby inhibiting their activities [10]. The above results revealed that exposure of cells to 10 μM **8** had antiproliferative effects on tumor cells, which accumulated in the G1 phase of the cell cycle, caused by the decreased activity of a key driver of S phase progression, cdk2 [11]. This suggests that 10 μM **8** could arrest the checkpoint of G1/S transition and inhibit cancer cells to freely enter into the next S phase.

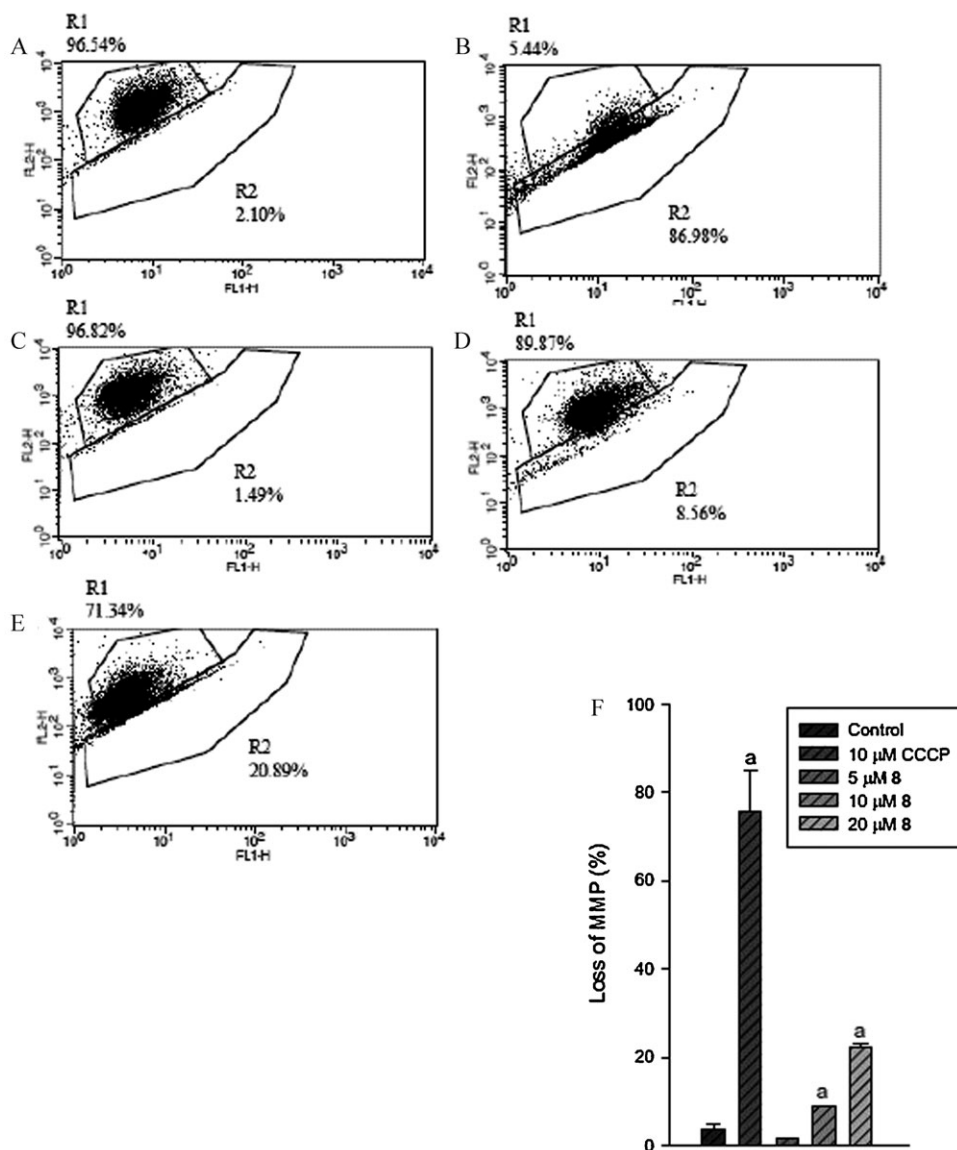


Figure 5. Collapse of MMP induced by CCCP and **8**. PC3 cells were treated without CCCP and **8** (control; A), 10 μ M CCCP (B), 5 μ M **8** (C), 10 μ M **8** (D), or 20 μ M **8** (E) for 24 h. Appropriate gates were made to define JC-1 aggregates (R1) and JC-1 monomers (R2). The bars (F) show the percentages of depolarized populations and the results are shown as the means \pm SD of triplicate experiments: $p < 0.05$ (a) compared to the respective control value.

Anti-apoptotic proteins (e.g., Bcl-2 and Bcl-xL) are essential for the regulation of apoptosis through caspase signaling [12]. Previous studies have exhibited that caspase-8 cleaves Bid to form tBid, which through direct correlation with an anti-apoptotic member of the Bcl-2 family releases pro-apoptotic Bax or Bak to generate pores in the mitochondrial membrane, leading to the cytochrome *c*-dependent caspase-3 pathway [13, 14]. Since Western blot analysis displayed that the expression levels of Bcl-2 and caspase-3 and -8 were decreased in response

to treatment with 20 μ M **8** (Fig. 6B), this may suggest that caspase-3 activation elicited by 20 μ M **8** might result from upstream caspases such as caspase-8. Thus, caspase-8 might play an initiating role.

Since an increase in the permeability of the outer mitochondrial membrane leads to the release of several apoptotic factors, such as cytochrome *c*, we investigated whether the apoptosis induced by 20 μ M **8** in PC3 cells involved the release of cytochrome *c*. Western blot analysis

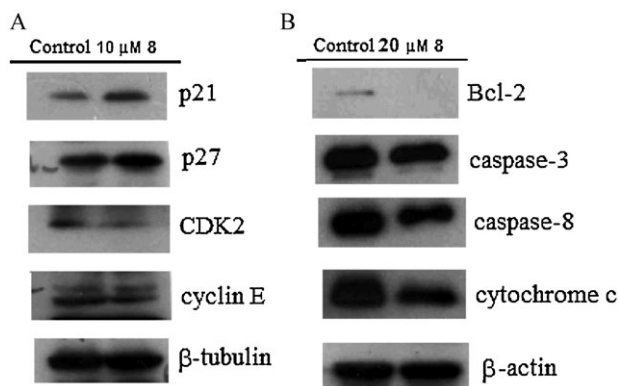


Figure 6. Compound **8** alters the expressions of proteins involved in the cell cycle and apoptosis. The levels of (A) cell cycle-related proteins (p21, p27, cdk2, and cyclin E) and (B) apoptosis-related proteins (Bcl-2, caspase-3, caspase-8, and cytochrome *c*) were determined in PC3 cells treated with vehicle (control) or 10 or 20 μM **8**, for 24 h. The Western blot analysis shown here is representative of three independent experiments with similar results. β-Tubulin and β-actin were employed as loading controls, respectively.

indicated that the level of cytochrome *c* in the mitochondria decreased upon treatment with 20 μM **8** and correlated with a decrease in the MMP (Figs. 5E, F and 6B).

Conclusion

In this study, we report on the design, synthesis, and biological evaluation of lantabetulic acid (**1**) and its derivatives. Most of the compounds displayed significant cytotoxic effects against human prostate cancer cells. The selective compound **8**, at concentrations of 5 and 10 μM, mainly induced cell death through the induction of G1 phase arrest in PC3 cells, while 20 μM **8** mainly induced cell death through the apoptotic pathway (which correlated with increased intracellular ROS generation), decreased the expression of Bcl-2 and caspase-8, induced mitochondrial changes and decreased the level of cytochrome *c* in mitochondria. This may also correlate with the decreased expression of caspase-3. The dual action of **8** could provide a new approach for the development of chemotherapeutic drugs.

Experimental

Reagents, starting material, and solvents were purchased from commercial suppliers. Cisplatin was obtained from Pharmacia Upjohn (Milan, Italy). All culture reagents were obtained from Gibco BRL. Optical rotations were recorded with a JASCO-370 polarimeter using CH₂Cl₂ as solvent. IR spectra were determined with a Perkin-Elmer system 2000 FTIR spectrophotometer. ¹H (400 MHz) and ¹³C (100 MHz) NMR spectra were recorded on

a Varian UNITY-400 spectrometer. Low-resolution mass spectra and high-resolution mass spectra data were obtained on a JMX-HX 100 mass spectrometer. Chromatography was performed using the flash-column technique on Silica Gel 60 supplied by E. Merck.

Chemistry

Extraction of lantabetulic acid (**1**)

Compound **1** was isolated from the roots of *R. javanica* L. var. *roxburghiana*. The structure was determined by various spectroscopic methods and compared to data reported in the literature [7].

Esterification at the C-17 carboxylic acid of **1**

Methyl 3,25-epoxy-3α-hydroxylup-20(29)-en-28-oate (2): To compound **1** (50 mg, 0.11 mmol) in CHCl₃ two drops of TMSCHN₂ were added. The reaction mixture was stirred at room temperature for 1 h. The mixture was concentrated to dryness under reduced pressure. The crude product was purified by chromatography using *n*-hexane/acetone (5:0.5) to give a colorless powder (21 mg, 0.04 mmol, 41%), [α]_D²⁵ 59 (c 0.1, CHCl₃), IR (KBr) cm⁻¹ 3390, 1724, 1639. ¹H NMR (CDCl₃) δ 0.83 (3H, s, Me-26), 0.94 (3H, s, Me-27), 0.95 (3H, s, Me-24), 1.01 (3H, s, Me-23), 1.67 (3H, s, Me-30), 2.97 (1H, dt, J = 10.8, 4.4 Hz, H_F-19), 3.65 (3H, s, COOCH₃), 3.71 (1H, d, J = 8.8 Hz, H_α-25), 4.22 (1H, d, J = 8.8 Hz, H_F-25), 4.60 (1H, brs, H_α-29), 4.72 (1H, brs, H_F-29). ¹³C NMR (CDCl₃) see Table 2. EIMS (70 eV) *m/z* (% rel. int.), 484 [M]⁺ (24). HREIMS *m/z* calcd. for C₃₁H₄₈O₄, 484.3552; found: 484.3534.

General procedure for the esterification at the C-17 carboxylic acid of **1**

To compound **1** (30 mg, 0.06 mmol) in acetone K₂CO₃ (6.39 mg, 0.05 mmol) and different alkyl halides or benzyl halide or 2-chloroethanol or α-monochlorohydrin (each at 0.3 mmol) was added. The reaction mixture was refluxed for 24 h. The mixture was concentrated to dryness under reduced pressure, diluted with 10% HCl solution, and extracted with EtOAc. The organic phase was dried over anhydrous Na₂SO₄, filtered, and concentrated *in vacuo* to give the crude product. The crude product was purified by chromatography using *n*-hexane/acetone as eluate to afford the purified compounds **3–8**.

Ethyl 3,25-epoxy-3α-hydroxylup-20(29)-en-28-oate (**3**)

Compound **3** was prepared from **1** (30 mg, 0.06 mmol) following the general procedure described for the esterification at the C-17 carboxylic acid of **1**, using ethyl iodide as alkyl halide moiety. Compound **3** was obtained as colorless powder (29.9 mg, 0.06 mmol, 94%), [α]_D²⁵ 52 (c 0.1, CH₂Cl₂), IR (KBr) cm⁻¹ 3392, 1719, 1640. ¹H NMR (CDCl₃) δ 0.83 (3H, s, Me-26), 0.93 (3H, s, Me-27), 0.95 (3H, s, Me-24), 1.00 (3H, s, Me-23), 1.24 (3H, t, J = 6.8 Hz, COOCH₂CH₃), 1.67 (3H, s, Me-30), 2.99 (1H, dt, J = 10.8, 4.4 Hz, H_F-19), 3.71 (1H, d, J = 8.8 Hz, H_α-25), 4.21 (1H, d, J = 8.8 Hz, H_F-25), 4.12 (2H, m, COOCH₂CH₃), 4.59 (1H, brs, H_α-29), 4.71 (1H, brs, H_F-29). ¹³C NMR (CDCl₃) see Table 2. EIMS (70 eV) *m/z* (% rel. int.), 498 [M]⁺ (90). HREIMS *m/z* calcd. for C₃₂H₅₀O₄, 498.3708; found: 498.3710.

2'-Hydroxyethyl 3,25-epoxy-3α-hydroxylup-20(29)-en-28-oate (**4**)

Compound **4** was prepared from **1** (30 mg, 0.06 mmol) following the general procedure described for the esterification at the C-17

carboxylic acid of **1** using 2-chloroethanol to substitute for the alkyl halide moiety. Compound **4** was obtained as colorless powder (25.9 mg, 0.05 mmol, 79%), $[\alpha]_D^{25}$ 28 (c 0.1, CHCl₃), IR (KBr) cm⁻¹ 3398, 1720, 1645. ¹H NMR (CDCl₃) δ 0.83 (3H, s, Me-26), 0.93 (3H, s, Me-27), 0.94 (3H, s, Me-24), 1.00 (3H, s, Me-23), 1.68 (3H, s, Me-30), 2.97 (1H, dt, *J* = 12.2, 6.8 Hz, H_β-19), 3.70 (1H, d, *J* = 8.8 Hz, H_α-25), 3.80 (2H, t, *J* = 4.8 Hz, COOCH₂CH₂OH), 4.20 (1H, d, *J* = 8.8 Hz, H_β-25), 4.21 (2H, m, COOCH₂CH₂OH), 4.59 (1H, brs, H_α-29), 4.71 (1H, brs, H_β-29). ¹³C NMR (CDCl₃) see Table 2. EIMS (70 eV) *m/z* (% rel. int.) 514 [M]⁺ (39). HREIMS *m/z* calcd. for C₃₂H₅₀O₅, 514.3658; found: 514.3646.

2',3'-Dihydroxypropyl 3,25-epoxy-3α-hydroxylup-20(29)-en-28-oate (5)

Compound **5** was prepared from **1** (30 mg, 0.06 mmol) following the general procedure described for the esterification at the C-17 carboxylic acid of **1** using α-monochlorohydrin to substitute for the alkyl halide moiety. Compound **5** was obtained as colorless powder (24.2 mg, 0.04 mmol, 74%), $[\alpha]_D^{25}$ 35 (c 0.1, CHCl₃), IR (KBr) cm⁻¹ 3391, 1722, 1641. ¹H NMR (CDCl₃) δ 0.83 (3H, s, Me-26), 0.94 (3H, s, Me-27), 0.95 (3H, s, Me-24), 1.00 (3H, s, Me-23), 1.67 (3H, s, Me-30), 2.96 (1H, dt, *J* = 11.6, 5.2 Hz, H_β-19), 3.60 (1H, m, COOCH₂CHOHCHHOH), 3.68 (1H, m, COOCH₂CHOHCHHOH), 3.72 (1H, d, *J* = 8.8 Hz, H_α-25), 3.90 (1H, m, COOCH₂CHOHCH₂OH), 4.11 (1H, d, *J* = 6.4 Hz, COOCHH-CHOHCH₂OH), 4.21 (1H, d, *J* = 8.8 Hz, H_β-25), 4.23 (1H, d, *J* = 6.4 Hz, COOCHHCHOHCH₂OH), 4.60 (1H, brs, H_α-29), 4.71 (1H, brs, H_β-29). ¹³C NMR (CDCl₃) see Table 2. EIMS (70 eV) *m/z* (% rel. int.) 544 [M]⁺ (43). HREIMS *m/z* calcd. for C₃₃H₅₂O₆, 544.3764; found: 544.3768.

Propyl 3,25-epoxy-3α-hydroxylup-20(29)-en-28-oate (6)

Compound **6** was prepared from **1** (30 mg, 0.06 mmol) following the general procedure described for the esterification at the C-17 carboxylic acid of **1** using propyl iodide as alkyl halide moiety. Compound **6** was obtained as colorless powder (27.6 mg, 0.05 mmol, 90%), $[\alpha]_D^{25}$ 57 (c 0.1, CHCl₃), IR (KBr) cm⁻¹ 3393, 1720, 1639. ¹H NMR (CDCl₃) δ 0.82 (3H, s, Me-26), 0.93 (3H, s, Me-27), 0.95 (3H, s, Me-24), 0.95 (3H, t, *J* = 7.2 Hz, COOCH₂CH₂CH₃), 1.00 (3H, s, Me-23), 1.64 (2H, m, COOCH₂CH₂CH₃), 1.68 (3H, s, Me-30), 2.99 (1H, dt, *J* = 10.8, 4.4 Hz, H_β-19), 3.70 (1H, d, *J* = 8.8 Hz, H_α-25), 4.02 (2H, m, COOCH₂CH₂CH₃), 4.21 (1H, d, *J* = 8.8 Hz, H_β-25), 4.59 (1H, brs, H_α-29), 4.71 (1H, brs, H_β-29). ¹³C NMR (CDCl₃) see Table 2. EIMS (70 eV) *m/z* (% rel. int.) 512 [M]⁺ (99). HREIMS *m/z* calcd. for C₃₃H₅₂O₄, 512.3865; found: 512.3871.

Isoropyl 3,25-epoxy-3α-hydroxylup-20(29)-en-28-oate (7)

Compound **7** was prepared from **1** (30 mg, 0.06 mmol) following the general procedure described for the esterification at the C-17 carboxylic acid of **1** using isopropyl iodide as alkyl halide moiety. Compound **7** was obtained as colorless powder (30.4 mg, 0.06 mmol, 99%), $[\alpha]_D^{25}$ 19 (c 0.1, CHCl₃), IR (KBr) cm⁻¹ 3396, 1716, 1650. ¹H NMR (CDCl₃) δ 0.83 (3H, s, Me-26), 0.93 (3H, s, Me-27), 0.94 (3H, s, Me-24), 1.00 (3H, s, Me-23), 1.21, 1.23 (6H, d, *J* = 3.2 Hz, COOCH(CH₃)₂), 1.67 (3H, s, Me-30), 3.00 (1H, dt, *J* = 6.8, 3.6 Hz, H_β-19), 3.70 (1H, d, *J* = 8.8 Hz, H_α-25), 4.21 (1H, d, *J* = 8.8 Hz, H_β-25), 4.58 (1H, brs, H_α-29), 4.71 (1H, brs, H_β-29), 4.99 (1H, m, COOCH(CH₃)₂). ¹³C NMR (CDCl₃) see Table 2. EIMS (70 eV) *m/z* (% rel. int.) 512 [M]⁺ (43). HREIMS *m/z* calcd. for C₃₃H₅₂O₄, 512.3865; found: 512.3864.

Benzyl 3,25-epoxy-3α-hydroxylup-20(29)-en-28-oate (8)

Compound **8** was prepared from **1** (30 mg, 0.06 mmol) following the general procedure described for the esterification at the C-17 carboxylic acid of **1** using benzyl bromide as alkyl halide moiety. Compound **8** was obtained as colorless powder (25.9 mg, 0.05 mmol, 77%), $[\alpha]_D^{25}$ 51 (c 0.1, CHCl₃), IR (KBr) cm⁻¹ 3393, 1721, 1646. ¹H NMR (CDCl₃) δ 0.65 (3H, s, Me-26), 0.91 (3H, s, Me-27), 0.95 (3H, s, Me-24), 1.00 (3H, s, Me-23), 1.67 (3H, s, Me-30), 3.00 (1H, dt, *J* = 10.8, 4.4 Hz, H_β-19), 3.69 (1H, d, *J* = 8.8 Hz, H_α-25), 4.19 (1H, d, *J* = 8.8 Hz, H_β-25), 4.59 (1H, brs, H_α-29), 4.71 (1H, brs, H_β-29), 5.11 (2H, d, *J* = 12.4 Hz, COOCH₂C₆H₅), 7.35 (5H, m, COOCH₂C₆H₅). ¹³C NMR (CDCl₃) see Table 2. EIMS (70 eV) *m/z* (% rel. int.) 583 [M+Na]⁺ (100). HREIMS *m/z* calcd. for C₃₇H₅₂O₄, 560.3865; found: 560.3870.

General procedure for the alkanoylation at the C-3 hydroxyl of 1

To compound **1** (30 mg, 0.06 mmol) in 2 mL pyridine different anhydrides of carboxylic acid (0.3 mL, 3.17 mmol) or different carboxylic acids (0.3 mL, 4.01 mmol) were added. The mixture was refluxed at 80 °C for 24 h, neutralized with saturated sodium carbonate solution, and extracted with EtOAc. The organic phase was concentrated *in vacuo* to give the crude product. The crude product was purified by chromatography using *n*-hexane/acetone as eluate to afford the purified compounds **9–13**.

3α-Acetoxy-3,25-epoxylup-20(29)-en-28-oic acid (9)

Compound **9** was prepared from **1** (30 mg, 0.06 mmol) following the general procedure described for the alkanoylation at the C-3 hydroxyl of **1** using acetic anhydride as anhydride moiety. Compound **9** was obtained as colorless powder (24.6 mg, 0.05 mmol, 80%), $[\alpha]_D^{25}$ 57 (c 0.1, CH₂Cl₂), IR (KBr) cm⁻¹ 1736, 1701, 1646. ¹H NMR (CDCl₃) δ 0.91 (3H, s, Me-26), 0.93 (3H, s, Me-27), 1.02 (3H, s, Me-24), 1.07 (3H, s, Me-23), 1.69 (3H, s, Me-30), 1.94 (3H, s, OCOCH₃), 3.00 (1H, dt, *J* = 10.8, 6.0 Hz, H_β-19), 4.07 (1H, d, *J* = 11.6 Hz, H_α-25), 4.21 (1H, d, *J* = 11.6 Hz, H_β-25), 4.61 (1H, brs, H_α-29), 4.73 (1H, brs, H_β-29). ¹³C NMR (CDCl₃) see Table 2. EIMS (70 eV) *m/z* (% rel. int.) 512 [M]⁺ (3). HREIMS *m/z* calcd. for C₃₂H₄₈O₅, 512.3502; found: 512.3511.

3,25-Epoxy-3α-propionoxylup-20(29)-en-28-oic acid (10)

Compound **10** was prepared from **1** (30 mg, 0.06 mmol) following the general procedure described for the alkanoylation at the C-3 hydroxyl of **1** using propionic acid as carboxylic acid moiety. Compound **10** was obtained as colorless powder (22.4 mg, 0.04 mmol, 87.1%), $[\alpha]_D^{25}$ 36 (c 0.1, CH₂Cl₂), IR (KBr) cm⁻¹ 1730, 1701, 1650. ¹H NMR (CDCl₃) δ 0.91 (3H, s, Me-26), 0.93 (3H, s, Me-27), 1.01 (3H, s, Me-24), 1.07 (3H, s, Me-23), 1.07 (3H, t, *J* = 4.8 Hz, OCOCH₂CH₃), 1.69 (3H, s, Me-30), 1.98 (2H, q, *J* = 7.2 Hz, OCOCH₂CH₃), 3.00 (1H, dt, *J* = 10.8, 4.4 Hz, H_β-19), 4.06 (1H, d, *J* = 11.6 Hz, H_α-25), 4.22 (1H, d, *J* = 11.6 Hz, H_β-25), 4.61 (1H, brs, H_α-29), 4.73 (1H, brs, H_β-29). ¹³C NMR (CDCl₃) see Table 2. EIMS (70 eV) *m/z* (% rel. int.) 526 [M]⁺ (4). HREIMS *m/z* calcd. for C₃₃H₅₀O₅, 526.3658; found: 526.3666.

3α-Crotonoxy-3,25-epoxylup-20(29)-en-28-oic acid (11)

Compound **11** was prepared from **1** (30 mg, 0.06 mmol) following the general procedure described for the alkanoylation at the C-3 hydroxyl of **1** using *N,N'*-dicyclohexylcarbodiimide (in pyridine) as substitute for pyridine and crotonic anhydride as anhydride

moiety. Compound **11** was obtained as colorless powder (22.3 mg, 0.04 mmol, 69%), $[\alpha]_D^{25}$ 49 (c 0.1, CH₂Cl₂), IR (KBr) cm⁻¹ 1731, 1698, 1639. ¹H NMR (CDCl₃) δ 0.90 (3H, s, Me-26), 0.93 (3H, s, Me-27), 1.01 (3H, s, Me-24), 1.06 (3H, s, Me-23), 1.68 (3H, s, Me-30), 1.98 (3H, m, OCOCH=CHCH₃), 2.99 (1H, dt, *J* = 10.8, 4.4 Hz, H_β-19), 4.05 (1H, d, *J* = 11.6 Hz, H_α-25), 4.22 (1H, d, *J* = 11.6 Hz, H_β-25), 4.61 (1H, brs, H_α-29), 4.73 (1H, brs, H_β-29), 5.14 (1H, d, *J* = 10.4 Hz, OCOCH=CHCH₃), 5.19 (1H, m, *J* = 10.4 Hz, OCOCH=CHCH₃). ¹³C NMR (CDCl₃) see Table 2. EIMS (70 eV) (% rel. int.) 538 [M]⁺ (7). HREIMS *m/z* calcd. for C₃₄H₅₀O₅, 538.3658; found: 538.3644.

Biological assays

Cell culture and MTT assay for cell viability

Human PC3 cells were maintained in RPMI 1640 medium supplemented with 10% fetal bovine serum (FBS), 100 U/mL penicillin-G, 100 μg/mL streptomycin, and 2 mM L-glutamine [15]. The cells were cultured at 37°C in a humidified atmosphere containing 5% CO₂. For evaluating the cytotoxic effects of the tested compounds and the positive control cisplatin, a modified 3-[4,5-dimethylthiazol-2-yl]-2,5-diphenyltetrazolium bromide (MTT; Sigma Chemical Co.) assay was performed [15]. Briefly, the cells were plated at a density of 1800 cells/well in 96-well plates and incubated at 37°C overnight before drug exposure. The cells were then cultured in the presence of graded concentrations of the tested compounds **1–11** and cisplatin (Pharmacia & Upjohn), at 37°C for 72 h, and various concentrations of **8** at 37°C for 24, 48, and 72 h. At the end of the culture period, 50 μL MTT (2 mg/mL in PB) was added to each well and allowed to react for 3 h. Following centrifugation of the plates at 1000g for 10 min, the medium was removed and 150 μL of DMSO was added to each well. The proportions of surviving cells were determined by absorbance spectrometry at 540 nm using an MRX (DYNEXCO) microplate reader. The cell viability was expressed as the percentage of the viable cells under control culture conditions. The IC₅₀ values of each group were calculated by the median-effect analysis and presented as means ± standard deviation (SD).

Quantitative analysis of intracellular ROS

Production of ROS was analyzed by flow cytometry as described previously [16]. Briefly, cells were plated and treated as indicated. Ten micromolar of 2,7-dichlorodihydrofluorescein diacetate (H₂DCFDA; Molecular Probes, Eugene, OR, USA) was added to the treated cells 30 min prior to harvesting. The cells were collected by trypsinization and washed with PBS. The green fluorescence of intracellular 2',7'-dichlorofluorescein (DCF) was then analyzed immediately by a FACScan flow cytometer with a 525-nm band pass filter (Becton Dickinson, Germany).

Apoptosis assays

Apoptosis was measured using an annexin V-FITC apoptosis detection kit (BD PharMingen, San Jose, CA, USA). Cells cultured in 6-cm dishes were trypsinized and collected by centrifugation. The cell pellet was washed, resuspended in 1× binding buffer, and stained with annexin V-FITC, as recommended by the manufacturer. Cells were also stained with PI to detect necrosis or late apoptosis. The distribution of viable (FITC/PI-negative), early apoptotic (FITC-positive/PI-negative), late apoptotic (FITC/PI-double positive), and necrotic (PI-positive, FITC-negative) cells was determined using a BD FACSAria flow cytometer (Becton Dickinson). The results are expressed as percent of total cells.

Flow cytometry analysis

The DNA content was determined following PI staining of the cells as previously described [17]. Briefly, 8 × 10⁵ cells were plated and treated with 20 μM cisplatin and various concentrations of **8** for 24 h. These cells were harvested by trypsinization, washed with 1× PBS, and fixed in ice-cold MeOH at -20°C. After overnight incubation, the cells were washed with PBS and incubated with 50 μg/mL PI (Sigma) and 50 μg/mL RNase A (Sigma) in PBS at room temperature for 30 min. The fractions of cells in each phase of the cell cycle were analyzed using a FACScan flow cytometer and CellQuest software (Becton Dickinson).

Measurement of the mitochondrial membrane potential

PC3 cells (3 × 10⁵) treated with 10 μM CCCP and different concentrations of **8** were incubated for 30 min with 1 μM of 5,5',6,6'-tetrachloro-1,1',3,3'-tetraethyl benzimidazolyl carbocyanine iodide (JC-1) (Molecular Probes) in culture medium. The resulting cells were washed three times with PBS and dislodged with trypsin-EDTA. Cells were collected in PBS/2% BSA, washed twice by centrifugation (800g, 5 min), and resuspended in 0.3 mL PBS/2% BSA for analysis by a FACSCalibur flow cytometer (Becton Dickinson). The cytometer settings were optimized for green (R1) and red (R2) fluorescence and the ratio of JC-1 aggregates (red fluorescence) to JC-1 monomers (green fluorescence) was calculated to represent the MMP [18].

Western blot analysis

Cells were harvested by trypsinization and resuspended in a suitable amount of PBS to adjust the cell numbers. The cells were mixed with an equal volume of 2× sample buffer and boiled twice for 10 min to denature the proteins. Cell extracts were separated by SDS-PAGE. The proteins were transferred to nitrocellulose membranes (Millipore, Billerica, MA, USA) using a semi-dry blotter. The blotted membranes were treated with 5% w/v skimmed milk in TBST buffer (100 mM tris-HCl pH 7.5, 150 mM NaCl, 0.1% Tween-20). The membranes were incubated with specific antibodies at 4°C overnight. The membranes were washed with TBST buffer and incubated with the secondary antibody at room temperature for another 1 h. Signals were detected by chemiluminescence ECL reagent after TBST washing and visualized on Fuji SuperRX film.

Monoclonal antibodies specific for β-actin and cytochrome *c* and antibodies against cyclin E, cdk2, cdk4, p21, p27, and β-tubulin were purchased from Santa Cruz Biotechnology (Santa Cruz, CA, USA). Bcl-2, caspase-3, and caspase-8 were purchased from Cell Signaling (Beverly, MA, USA).

Preparation of mitochondrial and cytosolic lysates

PC3 cells were washed with PBS, resuspended in ice-cold lysis buffer (250 mM sucrose, 20 mM N-(2-hydroxyethyl)piperazine-N'-(2-ethanesulfonic acid) (HEPES) pH 7.5, 10 mM KCl, 1.5 mM MgCl₂, 1 mM each of EGTA, EDTA, DTT, and PMSF, and 10 μg/mL each of leupeptin, aprotinin, and pepstatin A), and incubated for 20 min. The cells were centrifuged at 750g for 10 min at 4°C, and the supernatants were further centrifuged at 10,000g for 25 min at 4°C in order to prepare the cytosolic fraction. The remaining pellets were resuspended in lysis buffer and used as the mitochondrial fraction after centrifugation at 10,000g for 25 min [19].

Data analysis

Data were expressed as means \pm SD. Statistical analyses were performed using the Bonferroni t-test method after ANOVA for multigroup comparison and Student's t-test method for two-group comparison; $p < 0.05$ was considered to be statistically significant.

This work was supported by a grant from the National Science Council of the Republic of China (NSC 101-2320-B-037-038).

The authors have declared no conflict of interest.

References

- [1] H. Gronberg, *Lancet* **2003**, 361, 859–864.
- [2] D. Deeb, X. Gao, H. Jiang, B. Janic, A. S. Arbab, Y. Rojanasakul, S. A. Dulchavsky, S. C. Gautam, *Biochem. Pharmacol.* **2010**, 79, 350–360.
- [3] S. M. Kuo, *Crit. Rev. Oncog.* **1997**, 8, 47–69.
- [4] F. W. A. Barros, P. N. Bandeira, D. J. B. Lima, A. S. Meira, S. S. de Farias, J. R. Albuquerque, H. S. dos Santos, T. L. G. Lemos, M. O. de Moraes, L. V. Costa-Lotufu, C. do Ó Pessoa, *Bioorg. Med. Chem.* **2011**, 19, 1268–1276.
- [5] H. Y. Tu, A. M. Huang, B. L. Wei, K. H. Gan, T. C. Hour, S. C. Yang, Y. S. Pu, C. N. Lin, *Bioorg. Med. Chem.* **2009**, 17, 7265–7274.
- [6] K. W. Lin, A. M. Huang, T. C. Hour, S. C. Yang, C. N. Lin, *Bioorg. Med. Chem.* **2011**, 19, 4274–4285.
- [7] T. H. Lee, J. L. Chiou, C. K. Lee, Y. H. Kuo, *J. Chin. Chem. Soc.* **2005**, 52, 833–841.
- [8] N. K. Hart, J. A. Lamberton, A. A. Sioumis, H. Soares, *Aust. J. Chem.* **1976**, 29, 655–671.
- [9] R. Martin, E. Ibeas, J. Carvalho-Tavares, M. Hernandez, V. Ruiz-Gutierrez, M. L. Nieto, *PLoS ONE* **2009**, 4, e5975.
- [10] P. Pitchakarn, S. Suzuki, K. Ogawa, W. Pompimon, S. Takahashi, M. Asamoto, P. Limtrakul, T. Shirai, *Cancer Lett.* **2011**, 306, 142–150.
- [11] P. Kollár, T. Bárta, V. Závalová, K. Šmejkal, A. Hampl, *Br. J. Pharmacol.* **2011**, 162, 1534–1541.
- [12] V. Kirkin, S. Joos, M. Zornig, *Biochim. Biophys. Acta* **2004**, 1644, 229–249.
- [13] D. D. Newmeyer, S. Ferguson-Miller, *Cell* **2003**, 121, 481–490.
- [14] D. R. Green, J. C. Reed, *Science* **1998**, 281, 1309–1312.
- [15] T. C. Hour, J. Chen, C. Y. Huang, J. Y. Guan, S. H. Lu, C. Y. Hsieh, Y. S. Pu, *Anticancer Res.* **2000**, 20, 3221–3225.
- [16] Y. S. Pu, T. C. Hour, J. Chen, C. Y. Huang, J. Y. Guan, S. H. Lu, *Anticancer Drugs* **2002**, 13, 293–300.
- [17] A. M. Huang, C. Montagna, S. Sharan, Y. Ni, T. Ried, E. Sterneck, *Oncogene* **2004**, 23, 1549–1557.
- [18] X. J. Wu, T. Stahl, Y. Hu, F. Kassie, *J. Nutr.* **2006**, 136, 608–613.
- [19] Y. O. Son, J. A. Hitron, X. Wang, A. Chang, J. Pan, Z. Zhang, J. Liu, S. Wang, J. C. Lee, X. Shi, *Toxicol. Appl. Pharmacol.* **2010**, 245, 226–235.